

International RILEM Workshop on  
**Integral Service Life Modelling of  
Concrete Structures**

Guimarães, Portugal

5-6 November 2007

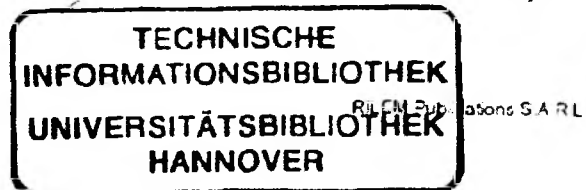
Edited by

**R.M. Ferreira**  
University of Minho, Portugal

**J. Gulikers**  
Ministry of Transport, Netherlands

and

**C. Andrade**  
Institute of Construction Sciences Eduardo Torroja – CSIC, Spain



## A TWO-SCALE APPROACH TO CONCRETE CARBONATION

S. A. Meier <sup>(1)</sup>, M. A. Peter <sup>(1)</sup>, A. Muntean <sup>(2)</sup>, M. Böhm <sup>(1)</sup> and J. Kropp <sup>(3)</sup>

(1) Centre for Industrial Mathematics, University of Bremen, Germany

(2) Department of Mathematics and Computer Science, TU Eindhoven, The Netherlands

(3) Institute for Building Materials, University of Applied Sciences, Bremen, Germany

### Abstract

We present a new approach of modelling the carbonation of concrete which accounts for diffusion processes on two different spatial scales. On the macroscopic scale, carbon dioxide is transported through the network of large capillary pores. On the microscopic scale, local transport and reaction take place in the small pores of the C-S-H gel phase. These processes are modelled on a representative unit cell by assuming an idealised, regular microstructure of the cement paste. Using a two-scale computational scheme, the model is validated by comparison with experimental data. It is examined under which conditions microscopic diffusion effects can play a significant role for the speed of the carbonation process.

Keywords: Carbonation, double-porosity, microstructure, mathematical modelling

### 1. INTRODUCTION

Many degradation mechanisms in cement-based materials are determined by diffusive transport of contaminants in the pore space. One of the most significant examples is the atmospheric carbonation of reinforced concrete [1]. Carbonation is caused by atmospheric  $\text{CO}_2$  diffusing through the pore space and reacting with dissolved  $\text{Ca}(\text{OH})_2$  (CH) in the pore water, which leads to a drop in pH. Since reaction and dissolution of the active species are fast compared to diffusion of  $\text{CO}_2$ , the process is mainly diffusion-controlled.

Several computational models have been developed for the prediction of the carbonation process. See, for instance, [2, 3, 4] and [5, 6]. An effect that is usually neglected in these and other modelling approaches is that diffusion in the pores of the hardened cement paste (hcp) actually happens at least on two different time and spatial scales: While the *fast* transport is mainly attributed to the large capillary pores, the  $\text{CO}_2$  also has to diffuse through the smaller pores in order to consume all available CH. If the larger capillary pores form a connected network, only the diffusion coefficient corresponding to the fast transport is determined by usual experiments. This can lead to an overestimation of the carbonation process, since not all of the CH can be reached by this latter type of transport. This effect has been proven to be significant for diffusion problems in fissured media and is effectively described by *double-porosity models*, which account for a hierarchical structure of the medium [7, 8].

In the present work, we formulate and test a *double porosity model with microstructure* for predicting the carbonation of concrete. We account for *macroscopic* diffusion of CO<sub>2</sub> in the capillary pore network and, simultaneously, for *microscopic* diffusion in the smaller pores of the C-S-H gel by assuming a regular geometrical structure of the cement paste. This two-scale system is conceptually similar to the one proposed in [9], in which the scale separation is attributed to the different magnitudes of the diffusivities of CO<sub>2</sub> in the gaseous and in the liquid phase. By comparison with experimental data from an accelerated carbonation test [10], we want to determine whether the double-porosity structure of the cement paste can be relevant for durability issues. We emphasise that the model presented is far from being complete, in the sense that effects like varying porosity and humidity and carbonation of phases other than CH are neglected. They can be added at a later stage in a similar fashion as has been already done for a conventional carbonation model proposed in [5, 6].

The two-scale computational scheme involving local representative unit-cells (RUCs) is strongly related to the mathematical theory of homogenisation [8]. A comprehensive theoretical study on homogenised carbonation models can be found in [11]. Similar schemes have been proposed for describing the mechanical behaviour of concrete [12]. We also note that the two-scale concept is not restricted to the prediction of carbonation, but can also be useful when modelling, for instance, moisture transport or hydration.

## 2. MICROSTRUCTURE OF CEMENT PASTE

### 2.1 Porosities and volume fractions

OPC cement paste consists of several solid phases and pores, whose radii vary over a wide spectrum from the nanometer to the micrometer scale. The amount and size of pores depend strongly on the water-to-cement ratio and on the hydration degree of the cement. In particular, if the cement has not completely hydrated, the capillary pores still form a connected network where most of the transport is located [13]. In contrast, the gel pores and smaller capillary pores allow only for very slow (local) transport and also for chemical reactions since they store most of the water due to their small radii.

In this work, we do not conceptually distinguish between capillary pores and gel pores, but consider only *large pores* (radius 0.05 – 1 μm) and *small pores* (radius 1 – 50 nm). For simplification, we assume that the cement paste is made up of unhydrated cement particles, the C-S-H gel and of large pores, with volume fractions  $\theta_u$ ,  $\theta_g$  and  $\theta_{lp}$ , respectively, referring to the volume of hcp, such that  $\theta_u + \theta_g + \theta_{lp} = 1$ . The C-S-H gel itself consists of C-S-H particles, CH crystals and small pores and has a porosity of  $\theta_{sp}$ . Other constituents of the C-S-H gel like other hydroxides or aluminate phases are neglected. The total porosity of hcp is therefore equal to  $\theta_g \cdot \theta_{sp} + \theta_{lp}$ . The *total porosity*  $\theta$  of the concrete is then

$$\theta = \theta_c (\theta_g \theta_{sp} + \theta_{lp}), \quad (1)$$

where  $\theta_c$  is the volume fraction of hcp referring to the total volume of concrete (see table 1 for some typical values).

## 2.2 Microscopic geometry

During hydration, C-S-H grains grow at the surface of the cement particles. Adopting the concept in [14], the unhydrated cement particles are idealised as spheres of a constant radius  $R_u = 7.4 \mu\text{m}$  forming a cubic lattice with periodicity  $l = 35 \mu\text{m}$  (figure 1). The particles are surrounded by the C-S-H gel, including CH crystals and small pores ( $R_g = 20.2 \mu\text{m}$ ). Thereby, we do not distinguish between inner and outer C-S-H and assume a constant porosity  $\theta_{sp}$  throughout the gel phase. The remaining space constitutes the connected network of large pores, which contributes to the total porosity via

$$\theta_{lp} = 1 - \frac{4\pi R_u^3}{3 l^3} \quad (2)$$

For detailed descriptions of the microstructure of cement paste we refer to [15, 13] and [16].

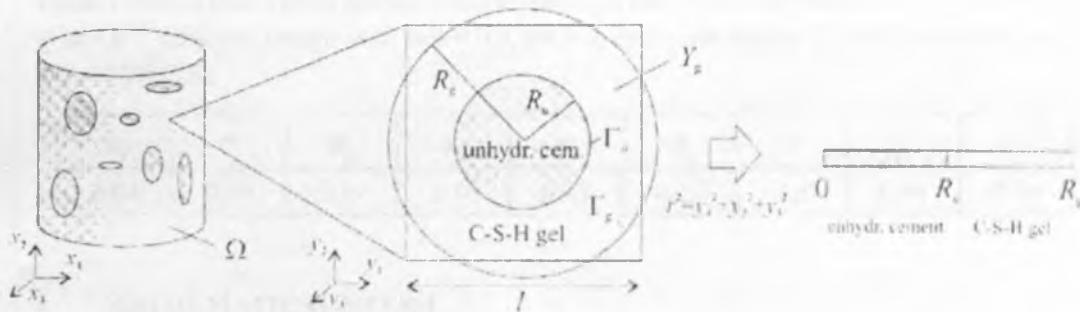
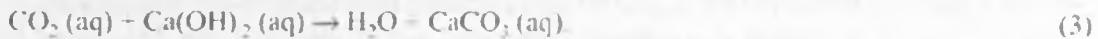


Figure 1: Idealised cement particle surrounded by C-S-H gel and transformation to 1D setting. The microscopic concentrations are defined on  $Y_g$ .

## 3. CARBONATION OF $\text{Ca}(\text{OH})_2$

The carbonation reaction of CH is usually described in a reduced form as



The reaction can only take place in water. If the relative humidity is less than about 85%, water will fill only the small pores by capillary condensation and will reside in the large pores only in form of vapour as well as condensed films along the pore walls [2]. Therefore, in our simplified model of the microstructure, the reaction is located in the C-S-H gel phase, which is supplied with gaseous  $\text{CO}_2$  from the large pores. Note that for higher humidity the model has to be extended by allowing carbonation also in the larger pores. Within the C-S-H gel, we adopt the carbonation model proposed in [10] with the following restrictions:

- Porosity change due to carbonation is excluded.
- Hydration reactions and carbonation of C-S-H are neglected.
- Dissolution of CH is instantaneous, such that the pore solution will stay saturated until all solid CH has been consumed.

Moreover, as in [10], the water saturation  $f$  of the small pores is assumed to be uniform and in steady state. In particular, the production of moisture by carbonation is neglected.

In order to clarify the notation, we remark that the *total water saturation*  $s$  of the concrete is related to  $f$  via

$$\theta \cdot s = \theta_c \theta_g \theta_{sp} \cdot f. \quad (4)$$

See table 1 for numerical values of the different saturation variables. Assuming that the reaction (3) takes place near the gas-liquid interfaces, its reaction rate is modelled as

$$r_{CH} = \theta_{sp} f^w H R T k_2 [\text{CH}]_{\text{eq}} [\text{CO}_2], \quad (5)$$

where  $f^w$  is the volume fraction of water in the small pores that is directly accessible by the air phase,  $H$  is the Henry constant of  $\text{CO}_2$ ,  $R$  the universal gas constant,  $T$  the temperature in Kelvin and  $k_2$  is the rate constant of reaction (3). Furthermore,  $[\text{CH}]_{\text{eq}}$  is the equilibrium concentration of aqueous CH and  $[\text{CO}_2]$  is the molar concentration of gaseous  $\text{CO}_2$ .

Table 1: Numerical values for the volume fractions and saturation variables. The values refer to an OPC concrete sample with  $w/c = 0.5$ ,  $a/c = 3$ , hydration degree 0.9 and uniform humidity  $\text{RH} = 65\%$  [16].

$\theta_u$	$\theta_g$	$\theta_{lp}$	$\theta_{sp}$	$\theta_c$	$\theta_g$	$s$	$f$	$f^w$
0.04	0.77	0.19	0.30	0.41	0.17	0.3	0.54	0.09

#### 4. MATHEMATICAL MODEL

We formulate the mathematical model on two scales: The key idea is to describe the fast (*global*) transport processes on a macroscopic scale while simultaneously resolving the slow (*local*) transport on a microscopic scale. This is established by coupling the macroscopic equations with local cell problems defined on the domain  $Y_g$  depicted in figure 1. In the present setting, the only fast diffusing species is  $\text{CO}_2$  in the large pores. Therefore, in the model equations we introduce two different mass concentrations for  $\text{CO}_2$  in the large pores ( $c_p^A$ ) and in the small pores ( $c_s^A$ ). See also table 2. The local spatial coordinate is denoted by  $y = (y_1, y_2, y_3) \in Y_g$ . The expressions  $c_p^A(x, y, t)$  and  $c_s^A(x, y, t)$  stand for the concentrations at time  $t$ , macroscopic space coordinate  $x$  and local space coordinate  $y$ .

Table 2: Mass concentrations ( $\text{kg}/\text{m}^3$ ) used in the two-scale model. For indexing, we abbreviate  $\text{CO}_2$  by  $A$  and CH by  $B$ .

Concentration	Notation	Defined for	Referring to
$\text{CO}_2$ in the large pores	$c_p^A(x, t)$	$x \in \Omega$	volume of large pores
$\text{CO}_2$ in the small pores	$c_s^A(x, y, t)$	$x \in \Omega, y \in Y_g$	volume of small pores
CH (solid)	$c_s^B(x, y, t)$	$x \in \Omega, y \in Y_g$	volume of C-S-H gel

#### 4.1 Macroscopic transport

On the *macroscopic scale*, concrete is regarded as an ideal mixture of aggregate and cement paste, having a total porosity  $\theta$  given by (1). We do not account for fissures or macroscopic pores at the interfaces between the aggregate and the binding material. However, the part of the porosity that is relevant for the macroscopic transport is only  $\theta_c \theta_p$ . The *mass balance of gaseous CO<sub>2</sub> in the large pores* reads

$$\frac{\partial}{\partial t} (\theta_c \theta_p c_{lp}^A) - \text{div}(\theta_c \theta_p D_{lp}^A \nabla c_{lp}^A) = -r_{gel}, \quad (6)$$

where  $-r_{gel}(x, t)$  denotes the amount of CO<sub>2</sub> that enters the C-S-H gel and is therefore lost in the mass balance within the large pores. This term is coupled with the local cell problems and is derived below. The initial condition is  $c_{lp}^A(x, 0)$ , while at the exposed surface we assume that  $c_{lp}^A$  equals the external CO<sub>2</sub> concentration  $c^{A,ext}$ .

#### 4.2 Microscopic transport and reaction

On the basis of the above assumptions, we now formulate the local mass balances for the active species in the C-S-H gel. The *mass balance of gaseous CO<sub>2</sub> in the small pores* is

$$\frac{\partial}{\partial t} (\theta_{sp} (1-f) c_{sp}^A) - \text{div}_y (\theta_{sp} (1-f) D_{sp}^A \nabla_y c_{sp}^A) = -(M^B)^{-1} r_{CH} \cdot H(c_s^B), \quad (7)$$

and that of *solid CH* is

$$\frac{\partial}{\partial t} c_s^B = -(M^A)^{-1} r_{CH} \cdot H(c_s^B) \quad (8)$$

Here,  $M^A$  and  $M^B$  are the molar weights, and the *Heaviside function*  $H(c_s^B)$  has the value 1 if  $c_s^B$  is greater than zero and 0 otherwise. At the interface  $\Gamma_g$ , we assume the CO<sub>2</sub> concentration to equal its corresponding value in the large pores, i.e.

$$c_{sp}^A = c_{lp}^A \quad \text{at } \Gamma_g \quad (9)$$

Since we consider no further exchange processes, all other interfacial conditions are zero-flux conditions. The initial conditions are  $c_{sp}^A(x, y, 0) = 0$  and  $c_s^B(x, y, 0) = c_s^{B,0}$ . Finally, the conservation of mass for CO<sub>2</sub> across the interface  $\Gamma_g$  gives the structure of the coupling term  $r_{gel}$  in (6), namely

$$r_{gel} = \frac{\theta_c}{\ell^3} \int_{\Gamma_g} [\text{diffusive flux of } c_{lp}^A] \cdot \nu \, d\sigma_r = \frac{\theta_c}{\rho^3} \int_{\Gamma_g} \theta_{sp} (1-f) D_{sp}^A \nabla_y c_{sp}^A \cdot \nu \, d\sigma_r \quad (10)$$

The effective diffusivity  $D_{lp}^A$  of CO<sub>2</sub> in the large pores is of order 10<sup>-8</sup> m<sup>2</sup>/s, while the value of  $D_{sp}^A$  is assumed to be of order 10<sup>-13</sup> m<sup>2</sup>/s [10]. For more details on the two-scale concept and a comprehensive analysis of the above model, see [17].

## 5. SIMULATION RESULTS

### 5.1 Numerical implementation

The coupled two-scale system (6)–(10) has been rescaled and implemented by the Finite-Element Method using COMSOL Multiphysics. By introducing spherical coordinates, the local cell problems for  $c_{sp}^A$  and  $c_s^B$  are reduced to one spatial dimension. In contrast to [9], they are not solved separately at each macroscopic integration point, but are embedded in a two-dimensional FE grid reflecting the two coordinates  $x$  and  $y$ . This reduces the assembling effort considerably. Within this structure, diffusion is allowed only in  $r$ -direction.

### 5.2 Verification by experimental data

In [10], accelerated laboratory carbonation tests are described, where hydrated or unhydrated OPC concrete samples are exposed to  $\text{CO}_2$  at a partial pressure of 0.5 bar and constant temperature of  $30^\circ\text{C}$  and relative humidity  $\text{RH} = 65\%$ . The concrete is assumed in moisture equilibrium throughout the process, which corresponds to a saturation degree of  $s = 0.3$ . We have tested our model for such a scenario with parameters referring to  $w/c = 0.5$  and  $a/c = 3$  (see also table 1). The boundary value for  $\text{CO}_2$  is  $c^{i,0} = 0.9 \text{ kg/m}^3$  and the initial value of CH is estimated by  $\theta_1, \theta_2, \theta_3^{0,0} = 117 \text{ kg/m}^3$  [16]

The resulting macroscopic concentration profiles are shown in figure 2. The movement of the carbonation front can be clearly seen from the steep gradients of the CH profiles in the right figure. Here, the average of CH over each cell is plotted, i.e., in spherical coordinates,

$$\langle c_s^B \rangle = \frac{4\pi}{\theta_1, \theta_2, \theta_3^{0,0}} \int_0^R r^2 c_s^B(x, r, t) dr \quad (11)$$

The local concentration profiles of  $\text{CO}_2$  and CH in the C-S-H gel are shown in figure 3, for three different positions within the sample. At  $x = 1.2 \text{ cm}$  (left figure), the concrete is completely carbonated and the CH concentration is zero. At  $x = 1.9 \text{ cm}$  (middle), CH ranges between 0 and 90% of its initial value. This inhomogeneity indicates that carbonation is in progress and is (at least partially) controlled by microscopic diffusion processes. At  $x = 2.4 \text{ cm}$  (right), carbonation has not yet started.

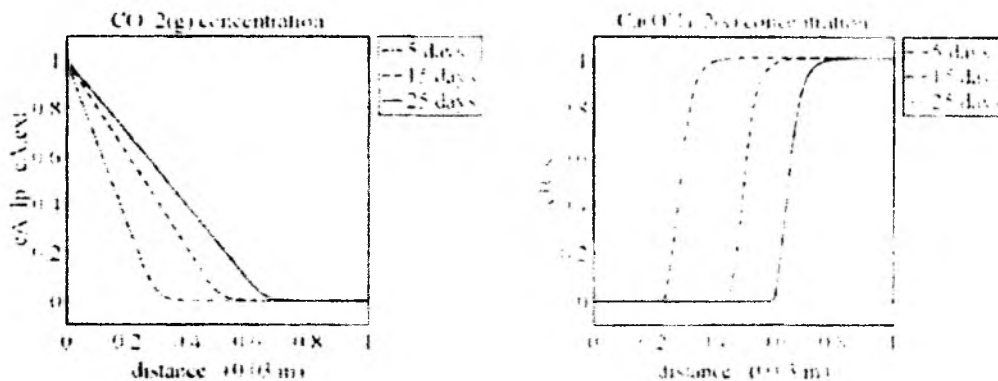


Figure 2: Concentration profiles of  $\text{CO}_2$  (left) and CH (right) within the concrete sample

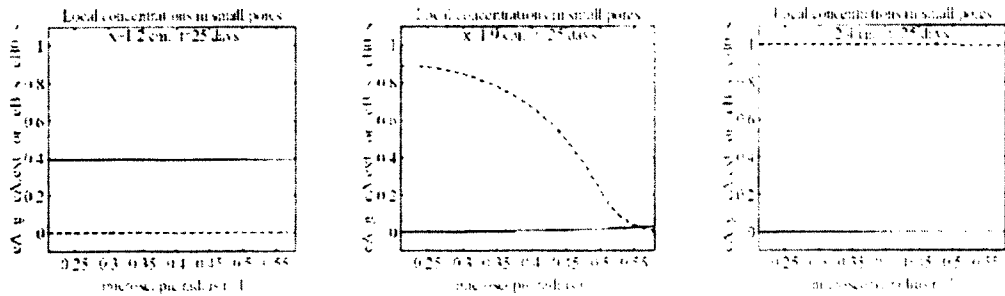


Figure 3: Microscopic cell profiles of  $\text{CO}_2$  (solid line) and  $\text{CH}$  (dashed) at different distances from the surface:  $x = 1.2$  cm (left),  $x = 1.9$  cm (middle) and  $x = 2.4$  cm (right).

The carbonation front, which we idealise by the position where the  $\text{CH}$  concentration has dropped to 10% of its initial value [2], is shown in figure 4 (left). There is a good agreement with the experimental values obtained in [10].

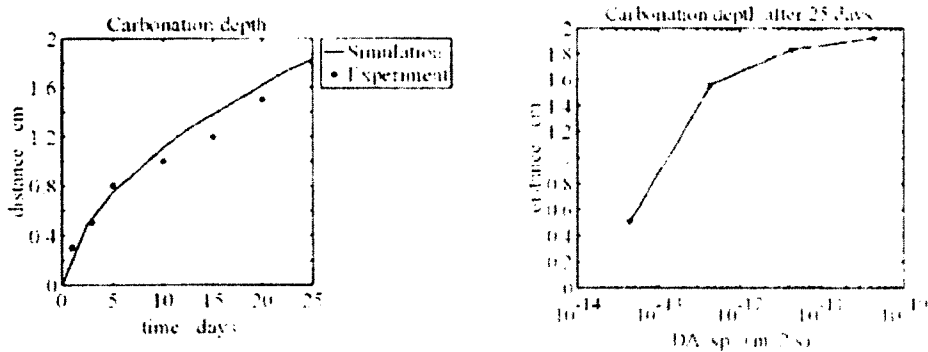


Figure 4: Left: Simulated carbonation depth and comparison with experimental values from [10]. Right: Parameter study with respect to the microscopic diffusivity  $D_m^{\text{CO}_2}$ .

### 5.3 Effect of microscopic diffusion

The microscopic diffusivity  $D_m^{\text{CO}_2}$  of  $\text{CO}_2$  in the C-S-H gel phase does not appear in classical carbonation models and its value is therefore a-priori unclear. Therefore, we perform a parameter study with respect to  $D_m^{\text{CO}_2}$  in order to highlight its effect on the process (figure 4, right). It can be seen that the carbonation depth after 25 days increases with increasing  $D_m^{\text{CO}_2}$ . For large diffusivities ( $D_m^{\text{CO}_2} > 10^{-11} \text{ m}^2/\text{s}$ ), an almost constant value is reached, which indicates that micro-scale diffusion is not relevant in this case. For smaller values of  $D_m^{\text{CO}_2}$ , the carbonation process is significantly reduced.

## 6. CONCLUSIONS

Carbonation of concrete has been modelled on two different length scales, accounting for a hierarchical double-porosity structure of the cement paste. The numerical tests using a two-scale computational scheme allow for the following conclusions:



- Experimental data can be recovered by the two-scale model.
- Local diffusion on the microscopic scale can have a significant effect on the carbonation process provided that the diffusivity is small enough compared to the macroscopic one.
- The numerical scheme works fine for one-dimensional geometries.

As a next step, the model can be extended to account for varying porosity, higher humidity (implying carbonation also in the larger pores) or carbonation of C-S-H. It is important to note that the two-scale modelling concept can conceptually distinguish between a reduction of small and of large pores. Hence, more accurate results are expected.

#### ACKNOWLEDGEMENTS

This work has been funded by the Deutsche Forschungsgemeinschaft (DFG) with a grant through the special priority program SPP1122. The support via the Ph.D. program *Scientific Computing in Engineering* as well as the German National Academic Foundation is also gratefully acknowledged.

#### REFERENCES

- [1] Kropp, J., 'Relations between transport characteristics and durability', in 'Performance criteria for concrete durability', Kropp, J. and Hilsdorf, H. K. (eds.) (E & FN SPON, 1995) 97–137.
- [2] Steffens, A., Dinkler, D. and Ahrens, H., 'Modeling carbonation for corrosion risk prediction of concrete structures', *Cem. Conc. Res.* 32 (2002) 935–941.
- [3] Sacca, A.V., Schrefler, B.A. and Vitaliani, R.V., '2-D model for carbonation and moisture / heat flow in porous materials', *Cem. Conc. Res.* 25 (1995) 1703–1712.
- [4] Bary, B. and Sellier, A., 'Coupled moisture-carbon dioxide-calcium transfer model for carbonation in concrete', *Cem. Conc. Res.* 34 (2004) 1859–1872.
- [5] Meier, S.A., Peter, M.A., Muntean, A. and Böhm, M., 'Dynamics of the internal reaction layer arising during carbonation of concrete', *Chemical Engineering Science* 62 (4) (2007) 1125–1137.
- [6] Peter, M.A., Muntean, A., Meier, S.A. and Böhm, M., 'Parametric study of the competition of several carbonation reactions in concrete' (Submitted for publication, 2006).
- [7] Arbogast, T., 'The double porosity model for single phase flow in naturally fractured reservoirs', in 'Numerical simulations in oil recovery', Wheeler, M. F. (ed.) (Springer, 1988) 23–45.
- [8] Hornung, U., 'Homogenization and Porous Media' (Springer, 1997).
- [9] Meier, S.A., Peter, M.A. and Böhm, M., 'A two-scale modelling approach to reaction–diffusion processes in porous materials', *Computational Materials Science* 39 (2007) 29–34.
- [10] Papadakis, V.G., Vayenas, C.G. and Fardis, M.N., 'A reaction engineering approach to the problem of concrete carbonation', *AIChE Journal* 35 (10) (1989) 1639–1650.
- [11] Peter, M.A., 'Coupled reaction–diffusion systems and evolving microstructure: mathematical modelling and homogenisation', PhD thesis, University of Bremen (Logos Verlag Berlin, 2007).
- [12] Löhnert, S. and Wriggers, P., 'Homogenisation of Microheterogeneous Materials Considering Interfacial Delamination at Finite Strains', *Technische Mechanik* 23 (2–4) (2003) 167–177.
- [13] Bier, T.A., 'Karbonatisierung und Realkalisierung von Zementstein und Beton', PhD thesis, University of Karlsruhe (1988).
- [14] Mackawa, K., Ishida, T. and Kishi, T., 'Multi-scale modeling of concrete performance. Integrated material and structural mechanics', *J. Adv. Concr. Tech.* 1 (2) (2003) 91–126.
- [15] Bentz, D.P. and Garboczi, E.J., 'Percolation of phases in a three-dimensional cement paste microstructural model', *Cem. Conc. Res.* 21 (2–3) (1991) 325–344.
- [16] Taylor, H.F.W., *Cement Chemistry* (Thomas Telford Publishing, 1997).
- [17] Meier, S.A., 'Two-scale models of reactive transport in porous media involving microstructural changes', PhD thesis, University of Bremen (2007, in preparation).